N93-18842

Optical Pathlength Control
on the JPL Phase B Interferometer Testbed

John Spanos and Zahidul Rahman

Jet Propulsion Laboratory, California Institute of Technology

Pasadena, California 91109

Abstract

Design and implementation of a controller for optical pathlength compensation on a flexible structure is presented. Nanometer level pathlength control is demonstrated in the laboratory. The experimental results are in close agreement with performance predictions.

Introduction

Many future space missions will require major advances in the areas of controlling, aligning, and pointing optical instruments mounted on large flexible structures. One of the most challenging applications is optical pathlength control for stellar interferometry [1]. Figure 1 shows one possible configuration of a long baseline interferometer with six collecting telescopes mounted on a free flying truss structure. The optics are designed such that any two collectors can be used as a stand-alone interferometer. For the interferometer to perform its mission successfully, the variations in the length of the path traveled by light through a pair of collectors to the detector (see Fig. 2) must be no more than a few nanometers [1].

Achieving nanometer level pathlength control becomes more difficult as optical elements are mounted on larger, more flexible structures. Loosely stated, the larger the distance separating the collecting apertures the better the astrometric accuracy of the interferometer. However, a longer baseline translates into a more flexible structure which in turn implies a more severe interaction between the structure and the feedback control system.

To meet the control structure interaction challenge, the Jet Propulsion Laboratory, in conjunction with a NASA–wide Control Structure Interaction (CSI) program, has developed the Phase B Testbed [2] in order to explore, develop, and validate emerging

technologies and design methodologies. In particular, JPL has initiated efforts toward a multilayer control approach involving (1) piezoelectric active member structural control, (2) active isolation control of on-board disturbances, and (3) direct control of optical elements. This paper addresses the optical control layer, presents the control system design methodology, and discusses the experimental results achieved.

The JPL Phase B Testbed

In order to address the control structure interaction problem associated with optical pathlength control, the Jet Propulsion Laboratory has developed a ground testbed facility known as the Phase B testbed (Fig. 3). This is an eight foot tall truss structure cantilevered at the base and equipped with an optical motion compensation system.* The optical compensation system is framed in a rectangular shaped trolley and attached firmly to the truss structure. A voice coil actuator and a piezoelectric (PZT) actuator provide high bandwidth pathlength control. Earlier control experiments conducted by O'Neal and Spanos [3] using an optical configuration that isolated most structural motion from the optical path demonstrated closed loop performance to the level of 11 nanometers rms. This paper describes the control system design and implementation for a new optical configuration that introduces a larger degree of coupling between structural motion and optical pathlength.

Figure 4 represents the current optical configuration and shows how laser interferometry was implemented in our experiment. Retroreflector and plane mirror interferometry were combined in such a way that the optical alignment is maintained under X and Z lateral motions and X, Y and Z rotational motions. This optical configuration is considerably less sensitive to alignment errors induced by structural vibration than either plane interferometry or retroreflector interferometry alone. In this setup the two laser beams are placed very close to each other and the returning beam is directed to the receiver by an additional plane mirror. Note that the laser beam passes eight times through the trolley as compared to two times with retroreflector interferometry or to four times with plane mirror interferometry.

Control Law Design

The frequency response functions (FRF) for the two input one output system were measured with a Tektronix 2630 Fourier analyzer and are shown in Figure 5. Sine sweep

---

* A detailed description of the Phase B testbed is given by Eldred and O'Neal [2].

and band limited white noise inputs were used to generate the FRF's with high coherence levels. The PZT actuator to laser pathlength FRF is not affected by the dynamics of the flexible structure due to the fact that the mass of the PZT mirror is small and the balanced PZT stack provides momentum compensation. Note that while the magnitude is relatively constant across the measured frequency band, the phase drops linearly with a constant slope corresponding to 70 microseconds of pure time delay. This delay is associated with the time it takes to measure the optical pathlength and output the measurement from the computer to the spectrum analyzer.

The voice coil to pathlength FRF is significantly affected by structural flexibility. The dominant peak at 0.7 Hz is due to the flexure that attaches the trolley to the truss. All other peaks in the frequency response function correspond to structural modes of the truss. Observe that the peaks and valleys (i.e., poles and zeroes) in the FRF are alternating up to 80 Hz which guarantees that all the modes below this frequency will interact stably with a controller of the phase lead type. Beyond 80 Hz the phase drops rapidly while modal density and plant uncertainty increase considerably. As a result, we have chosen to limit the bandwidth of the voice coil controller to a frequency lower than 80 Hz.

The architecture of the two-input one-output optical pathlength control system is shown in Figure 6. Bode's classical control design methods [4] were used to shape the open loop response in the frequency domain. We point out that, unlike most modern control design methods, this design methodology does not require an explicit parametric model of the plant using instead the FRF measurement directly to synthesize robust controllers.

The control system architecture is similar to that of Colavita [5] in the sense that the output of the PZT controller drives both the PZT actuator and the voice coil controller. The objective of this configuration is to desaturate the limited stroke PZT actuator in the low frequency range where disturbances tend to have large amplitudes. Note that in Fig. 6 we have modeled the PZT-to-pathlength transfer function as unity while the measurement in Fig. 5 shows it to be approximately 4.5 dB or 1.7. We shall compensate for this simplification later by dividing the PZT controller $K_1(s)$, and multiplying the voice coil controller $K_2(s)$ by a factor of 1.7 after the two control laws are designed.

The open loop transfer function for the system of Fig. 6 is

$$L = K_1 (1 + K_2 G_2) \tag{1}$$

The objective is to design the two compensators $K_1(s)$ and $K_2(s)$ such that the closed loop system is stable and the total loop gain $|L|$ is as large as possible over the largest achievable bandwidth. The design requirements are placed on $|L|$ since the disturbance rejection is inversely proportional to $|L|$ when $|L|$ is much larger than unity. The following three properties are observed from (1):

1. When $|K_2 G_2| \gg 1$, $|L| \approx |K_1 K_2 G_2|$
2. When $|K_2 G_2| \ll 1$, $|L| \approx |K_1|$
3. When $|K_2 G_2| = 1$, $|L| \approx \phi |K_1|$

where $\phi = angle(K_2 G_2) + \pi$ and $angle(K_2 G_2)$ is the phase angle (in radians) of $K_2 G_2$ at the frequency where $|K_2 G_2| = 1$. Clearly, when the voice coil loop gain is large, the total loop gain is the product of the voice coil loop gain and the PZT loop gain. The total loop gain also approaches the PZT loop gain as the voice coil loop gain approaches zero. Also at the voice coil loop gain crossover frequency the total loop gain is the product of the PZT loop gain and the phase margin ϕ associated with the voice coil loop.

The control laws were designed one loop at a time. First, the voice coil controller was designed to stabilize the system assuming that it is driven directly by the laser path-length measurement (i.e., $K_1(s)=1$) and the PZT actuator is disconnected. Using frequency domain loop shaping techniques, a voice coil controller with the following transfer function was obtained:

$$K_2(s) = (0.117) \underbrace{\left(\frac{s^2 + 245s + 204^2}{s^2 + 371s + 309^2} \right)}_{\text{LEAD}} \underbrace{\left(\frac{1,005^2}{s^2 + 402s + 1,005^2} \right)}_{\text{LOW PASS}} \underbrace{\left(\frac{s^2 + 50s + 503^2}{s^2 + 100s + 503^2} \right)}_{\text{NOTCH}}$$

The controller consists of (1) a second order lead filter that provides more than 30 degrees of phase at the gain cross over frequency, (2) a second order low pass filter that attenuates the high frequency lighly damped structural modes, and (3) a second order notch filter that attenuates the peak at 80 Hz so that the gain margin of the corresponding mode is approximately 6 dB. The low pass and notch filters are essential in ensuring a stable control structure iteration. The compensated voice coil to laser pathlength frequency response function is shown in figure 7.

Similarly, the transfer function of the PZT controller was designed:

$$K_1(s) = (3,137) \underbrace{\left(\frac{s + 378}{s} \right)}_{\text{LAG}} \underbrace{\left(\frac{s + 4,000}{s^2 + 440s + 394,784} \right)}_{\text{LOW PASS}}$$

The first order lag keeps the total loop gain high at low frequencies for good disturbance rejection. On the other hand, the second order low pass filter enforces a steep gain roll-off while maintaining adequate phase margin for stability robustness. Although the PZT actuator has very high bandwidth, the PZT loop bandwidth is limited by high frequency noise, digital implementation time delay, and phase lag from the power amplifier.

Figure 8 shows the loop transfer function L as well as the PZT controller K_1. The effects of time delays due to the computer implementation have been taken into account. The frequency responses are clearly in agreement with the three properties described earlier.

Both control laws were discretized using the bilinear transformation and prewarping was used to match them to their analog counterparts at the respective gain crossover frequencies. The low bandwidth voice coil controller and the high bandwidth PZT controller were implemented at 2,000 Hz and 12,000 Hz respectively. The phase lags associated with the zero order hold and the computational delay were modelled as pure time delays since the sampling frequencies of both controllers are much higher than their respective bandwidths.

Experimental Results

Two closed loop experiments were carried out. The objective of the first was to reject the ambient laboratory disturbance environment and to establish the noise floor of the closed loop system. The objective of the second was to reject a sinusoidal disturbance tuned to the frequency of the fundamental truss mode (i.e., 5.3 Hz). The sinusoidal disturbance was induced by a proof-mass type shaker attached to the midspan of the truss via a stinger.

In both experiments, the open loop optical pathlength histories were recorded for the first 5 seconds at which time the control loop was closed and the closed loop pathlength histories were recorded for an additional 5 seconds. The results from the experiments are shown in Figures 9 and 10.

Figure 9 shows the optical pathlength variation reduced to 24 nanometers rms from an open loop ambient disturbance of 15 micrometers rms. This corresponds to 56 dB rejection of the ambient disturbance. It is emphasized that in these experiments the laser beam makes 8 passes through the trolley optics which implies that the equivalent path-

length error for a space interferometer (i.e., Figures 1 and 2) would be 3 nanometer rms. Spectral analysis of the open and closed loop signals indicates that the achieved controller bandwidth is approximately 500 Hz and that a large part of the closed loop error is due to noise at frequencies beyond the controller bandwidth.

Figure 10 illustrates the forced response experiment. The impact of the 5.3 Hz sinusoidal disturbance on the pathlength is clearly shown during the first 5 seconds of the time history. The closed loop response indicates that the disturbance is attenuated by more than 70 dB which is in close agreement with the total loop gain of Figure 8.

Conclusions and Future Work

We have successfully designed and implemented a two input one output optical pathlength control system on an experimental flexible structure. The control design was carried out in the frequency domain by directly shaping the measured actuator-to-sensor frequency response function and did not require a parametric model of the system. Experiments were conducted to reject the laboratory ambient disturbance environment and also shaker induced disturbances tuned to the fundamental structural frequency. The results we have obtained so far indicate that nanometer level control of optical pathlength is feasible in space.

Presently we are reconfiguring the optical path in order to introduce a stronger coupling between the optical pathlength and the structure. The laser beam will be reflected back from an additional point on the structure where large structural motion has been observed. We are also in the process of introducing additional layers of control (i.e., passive/active damping, and disturbance isolation) to improve the overall performance of the pathlength compensation system.

Acknowledgements

References

[1] Laskin R. A., and San Martin A., "Control/Structure System Design of a Spaceborne Optical Interferometer", AAS/AIAA Astrodynamics Specialist Conference, 1989.

[2] Eldred D. B., and O' Neal M. C., "The JPL Phase B Testbed Facility", ADPA Active Materials & Adaptive Structures Symposium & Exhibition, 1991.

[3] O'Neal M. C., and Spanos J. T., "Optical Pathlength Control in the Nanometer Regime on the JPL Phase B Interferometer Testbed" SPIE Intl Symposium on Optical Applied Science and Engineering, 1991.

[4] Bode, H. W., *Network Analysis and Feedback Amplifier Design*, Van Nostrand, NY, 1945.

[5] Colavita, M. M., et al, "Prototype High Speed Optical Delay Line for Stellar Interferometry", SPIE Intl Symposium on Optical Applied Science and Engineering, 1991.
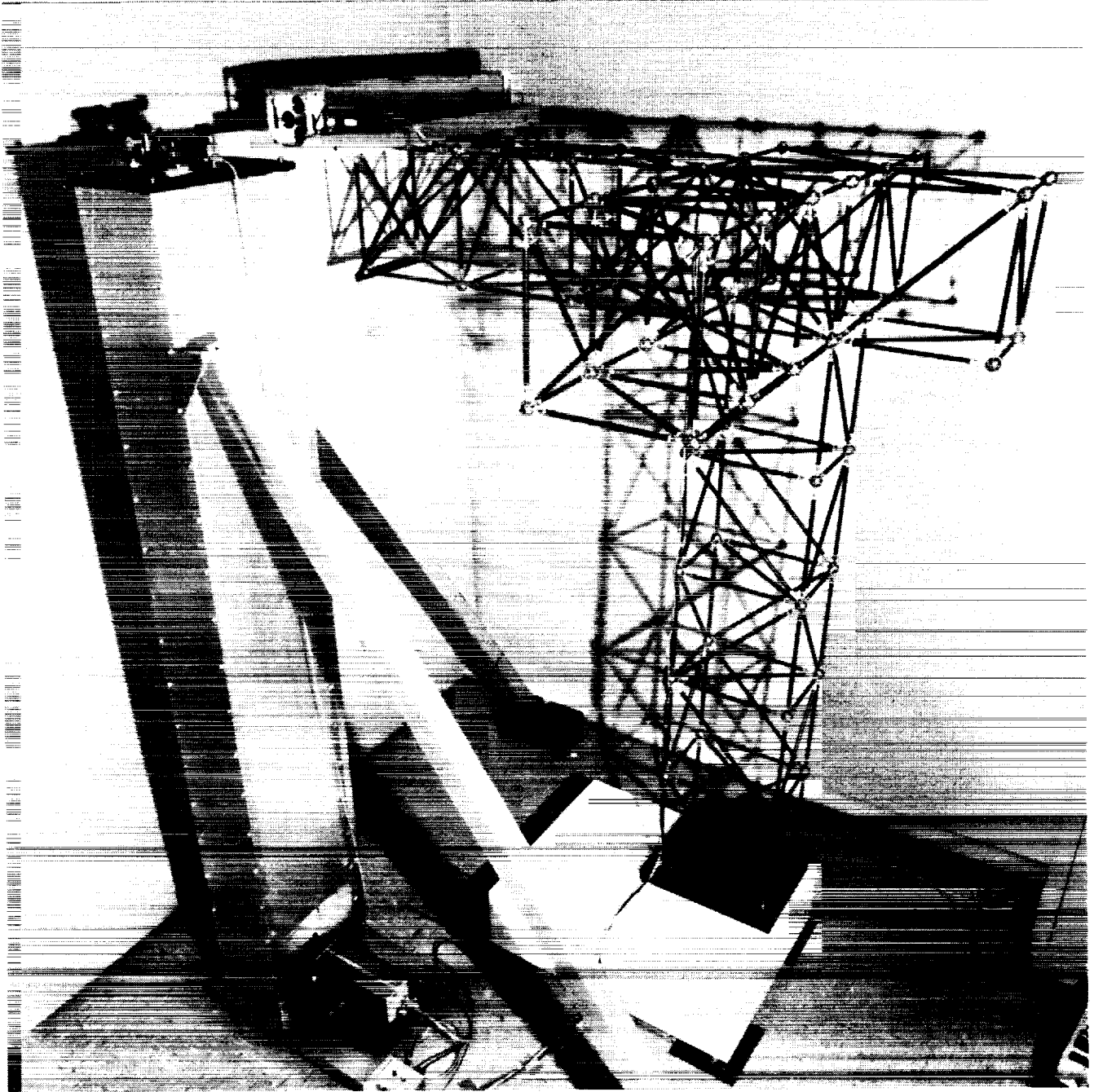
Figure 1. CSI Focus Mission Interferometer

LIGHT FROM STAR

SIDEROSTAT
- TIP/TILT (COARSE)
- RETROREFLECTOR MOUNTED IN CENTER

1

LIGHT FROM STAR

1'

COLLECTING SCOPE
- 0.5 m APERTURE
- 8:1 BEAM COMPRESSION
- OFFSET SECONDARY

3

THREE TIER TROLLEY
- TIMING BELT: 8 m RANGE
- VOICE COIL : 2 mm RANGE
- PZT STACK : 5 μm RANGE

3'

2

2'

FAST STEERING MIRROR
- TIP/TILT (FINE)
- REACTIONLESS

4

5

PZT STACK →

6

VOICE COIL

7

FRINGE TRACKER
Δ PATHLENGTH

8

TIMING BELT

9

9'

ANGLE TRACKER
Δ WAVETILT

8'

4'

5'

6'

7'

DETECTOR

COMBINING OPTICS
- BEAM SPLITTER AT BEND 9
- UP TO BENDS 8 AND 8', BOTH BEAMS EXPERIENCE IDENTICAL (NOT SYMMETRICAL) REFLECTIONS

FIXED TROLLEY
- MIMICS LIGHT BENDS OF MOVING TROLLEY

Figure 2. Optical Layout of an Interferometer

CSI FOCUS MISSION INTERFEROMETER
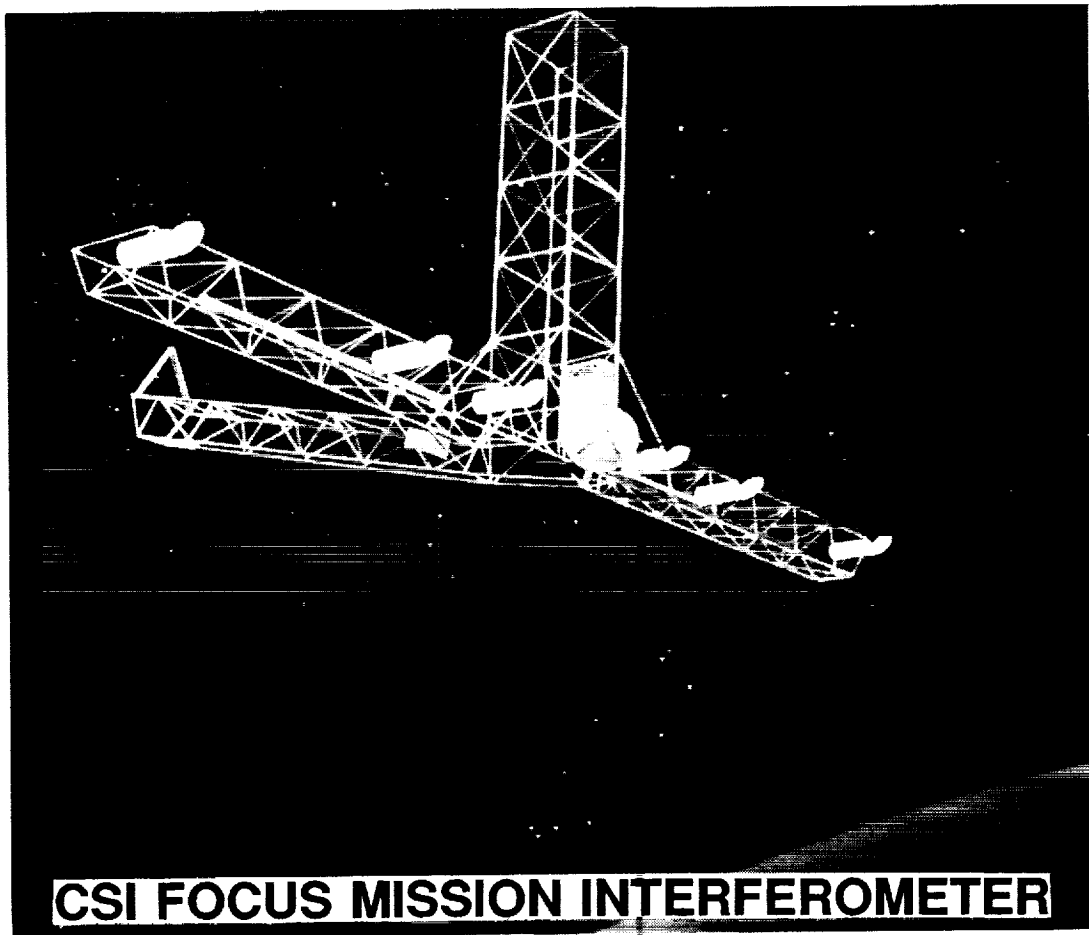
Figure 3. JPL CSI Phase B Testbed
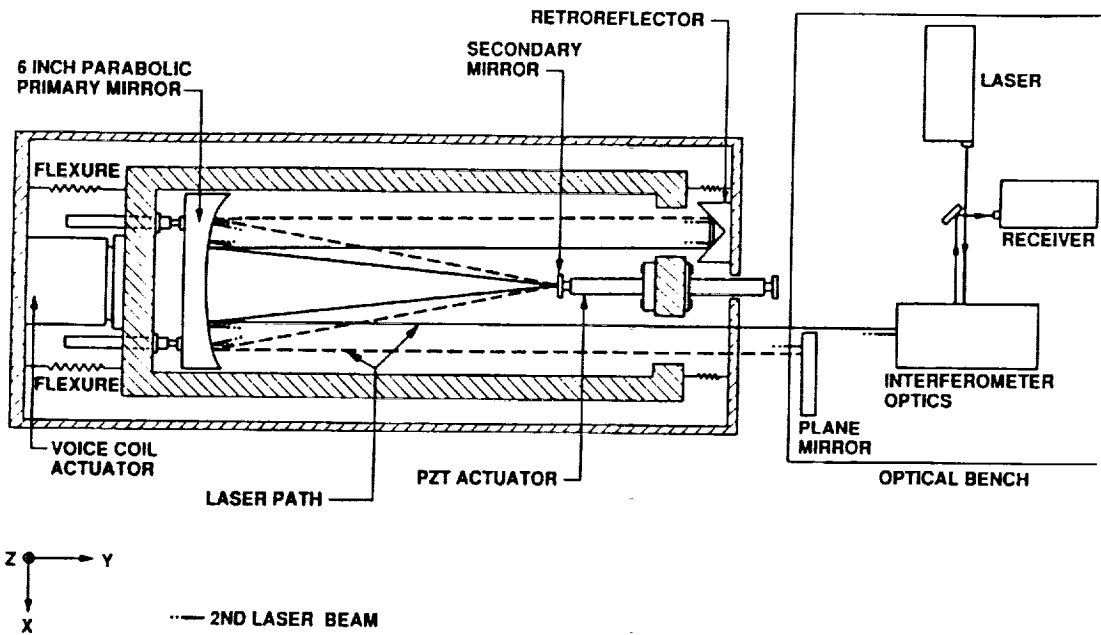
Figure 4. Optical Pathlength Compensation System
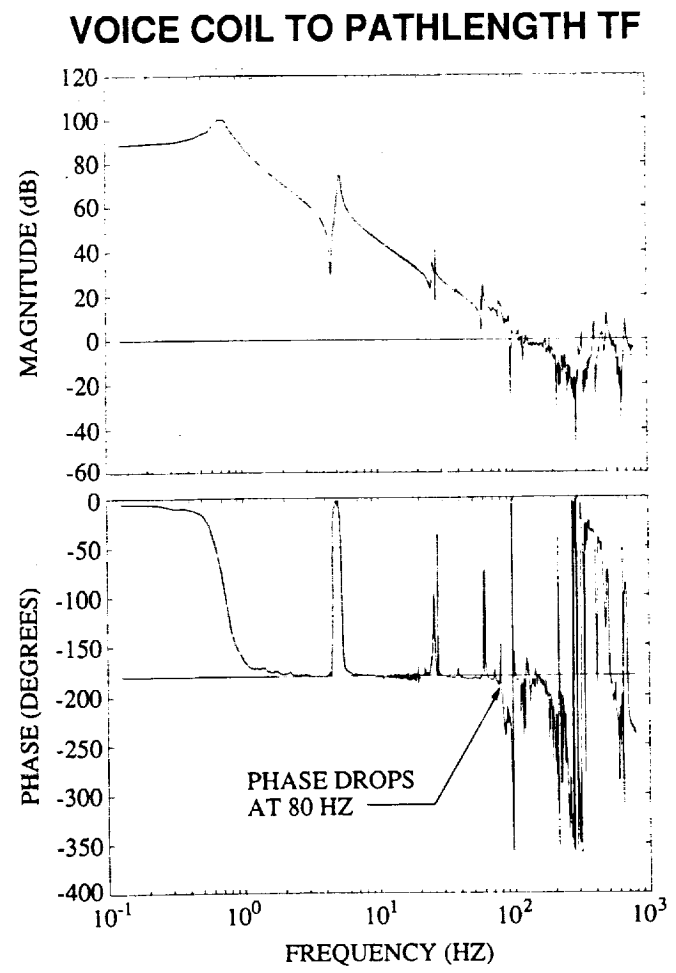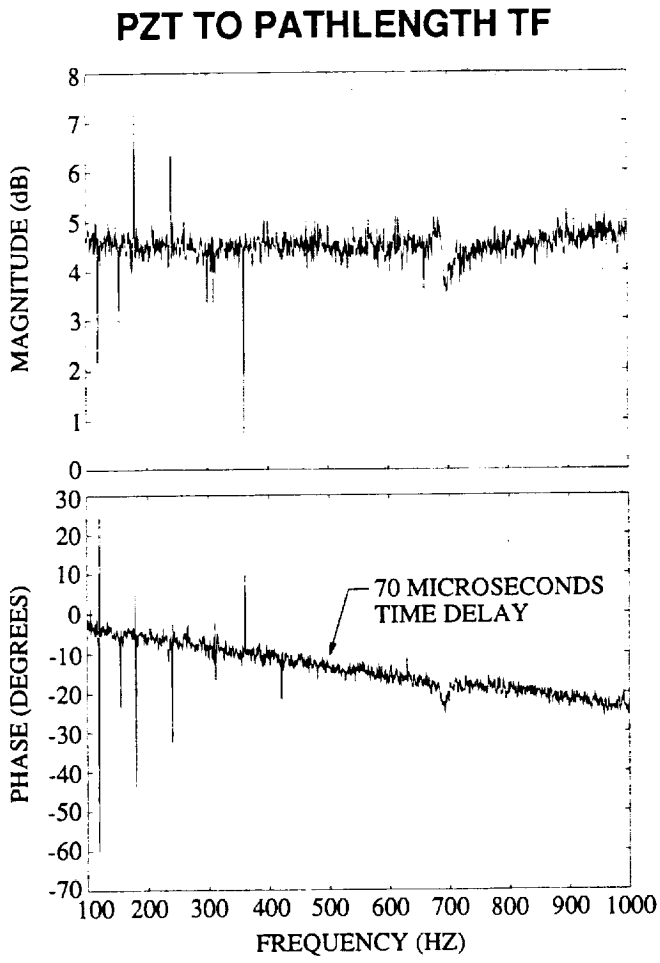
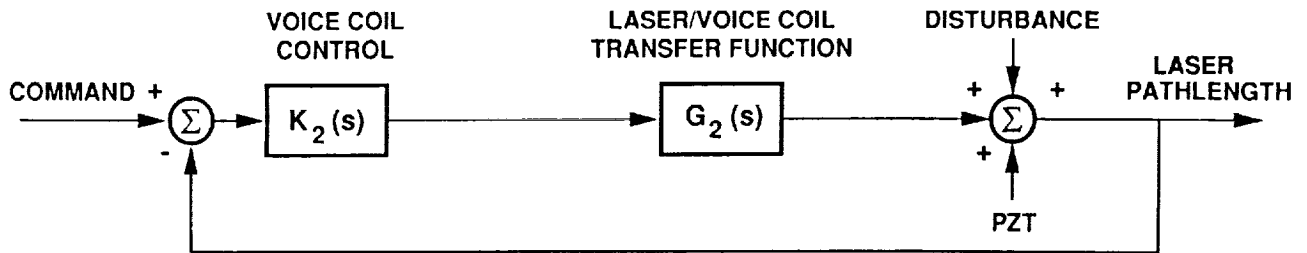**Figure 5.** Identified Frequency Response Functions
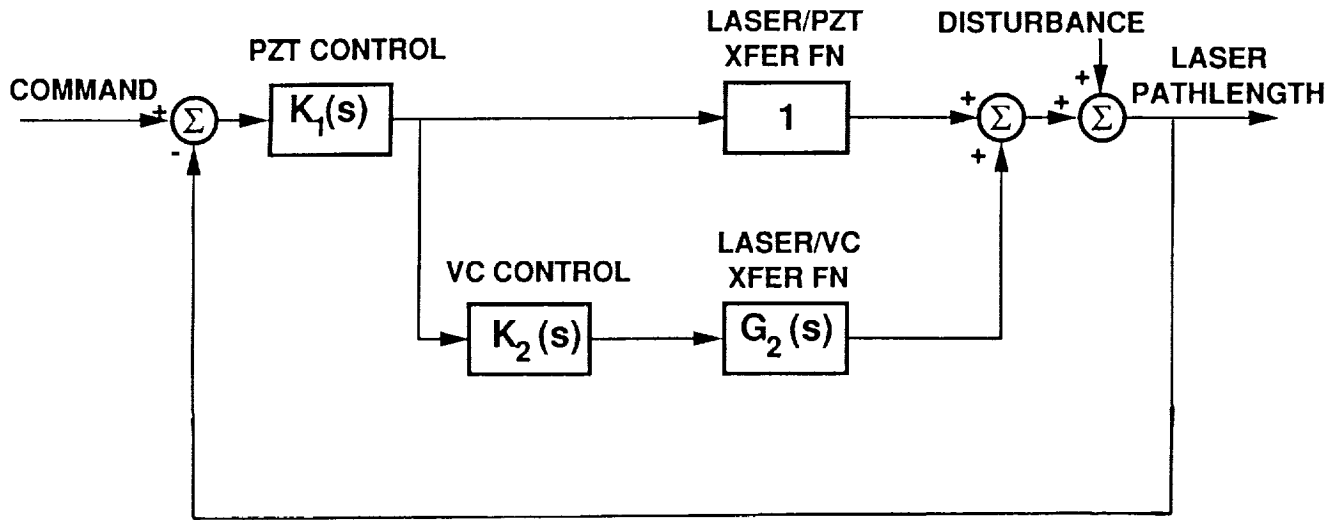
Figure 6. Control System Architecture

$$K_2(s) \;=\; (0.117) \; \underbrace{\left(\frac{s^2 + 245s + 204^2}{s^2 + 371s + 309^2} \right)}_{\text{LEAD}} \underbrace{\left(\frac{1,005^2}{s^2 + 402s + 1,005^2} \right)}_{\text{LOW PASS}} \underbrace{\left(\frac{s^2 + 50s + 503^2}{s^2 + 100s + 503^2} \right)}_{\text{NOTCH}}$$
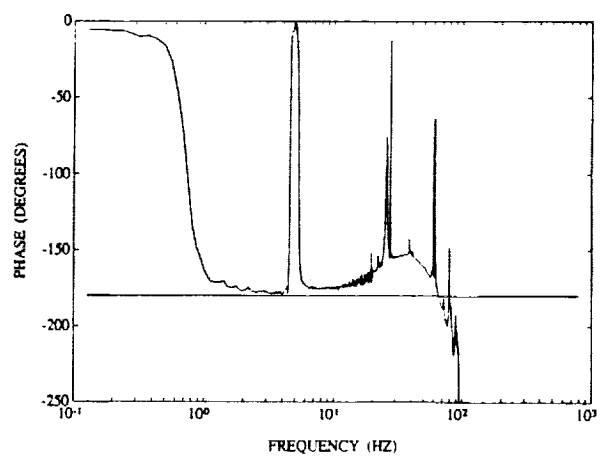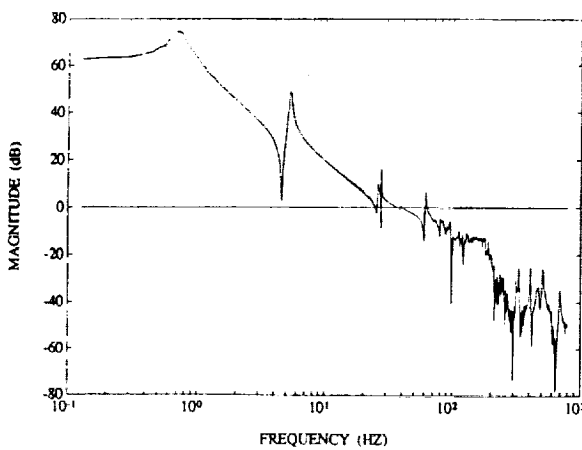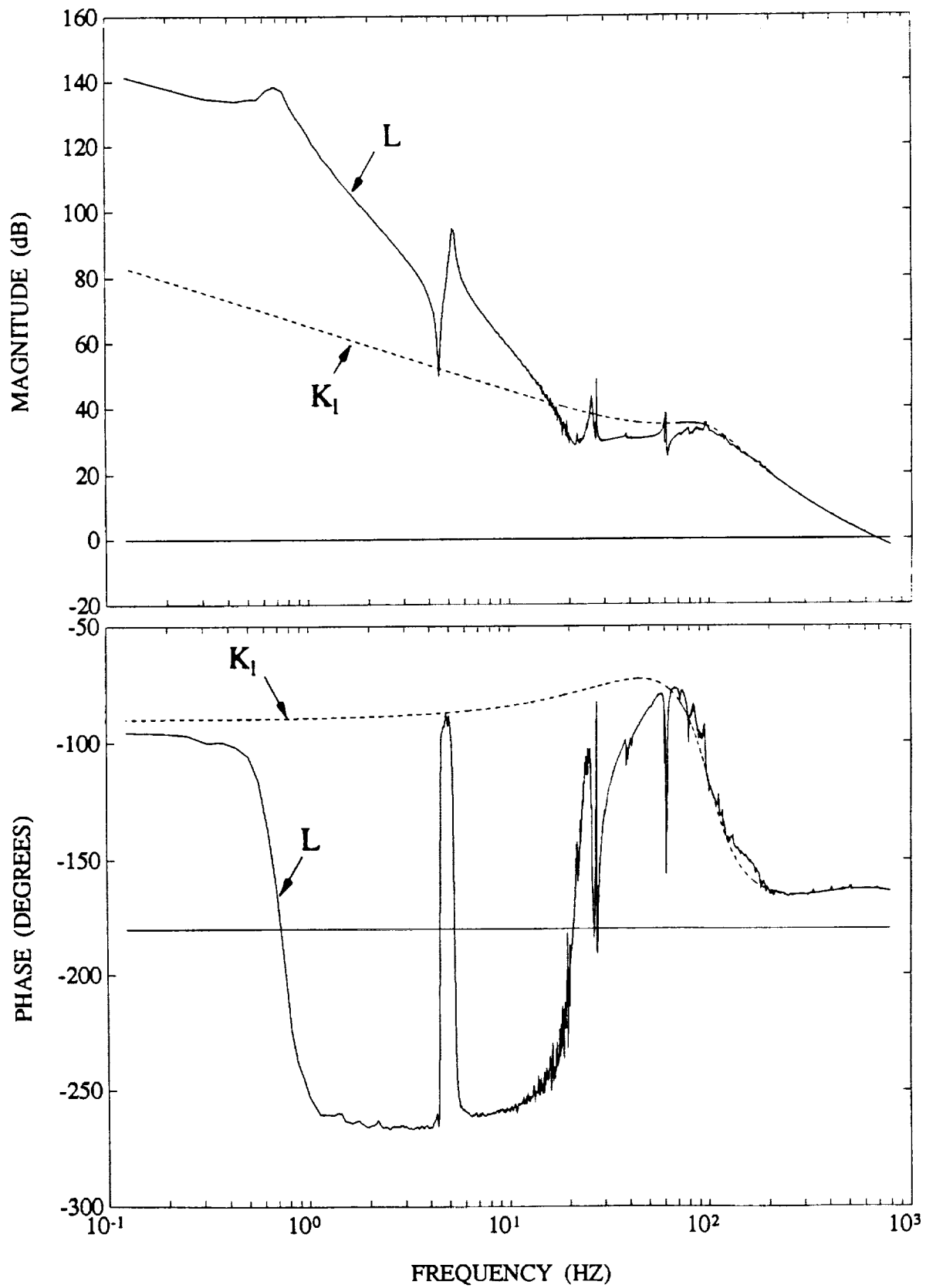

Figure 7. Voice Coil Loop Gain and Phase

Figure 8. PZT and Total Loop Gain and Phase

DISTURBANCE: LABORATORY ENVIRONMENT

OPEN LOOP: 15.2481 um RMS

CLOSED LOOP: 23.9999 nm RMS

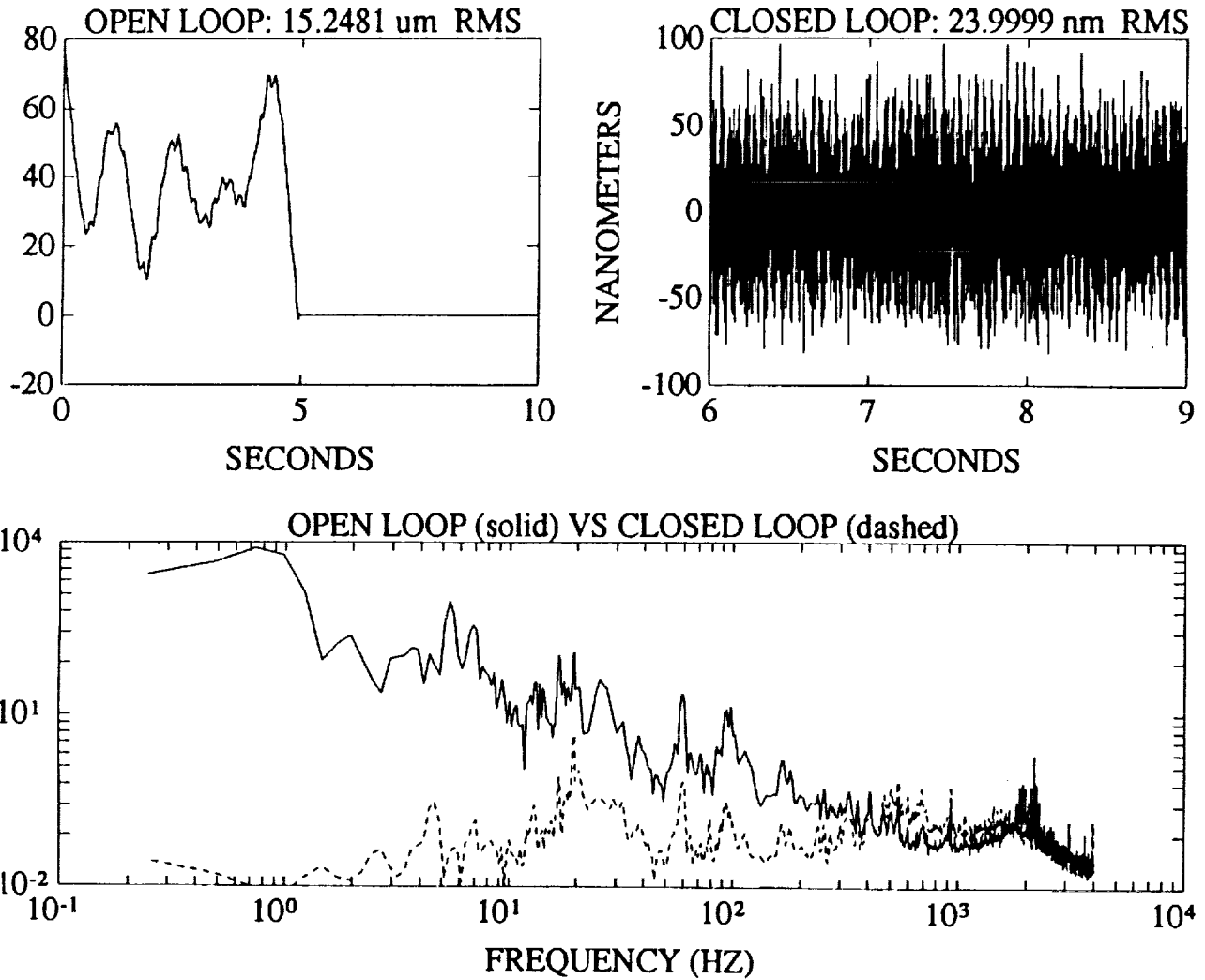OPEN LOOP (solid) VS CLOSED LOOP (dashed)

Figure 9. Closed Loop Optical Performance with Ambient Laboratory Disturbance

356

DISTURBANCE:
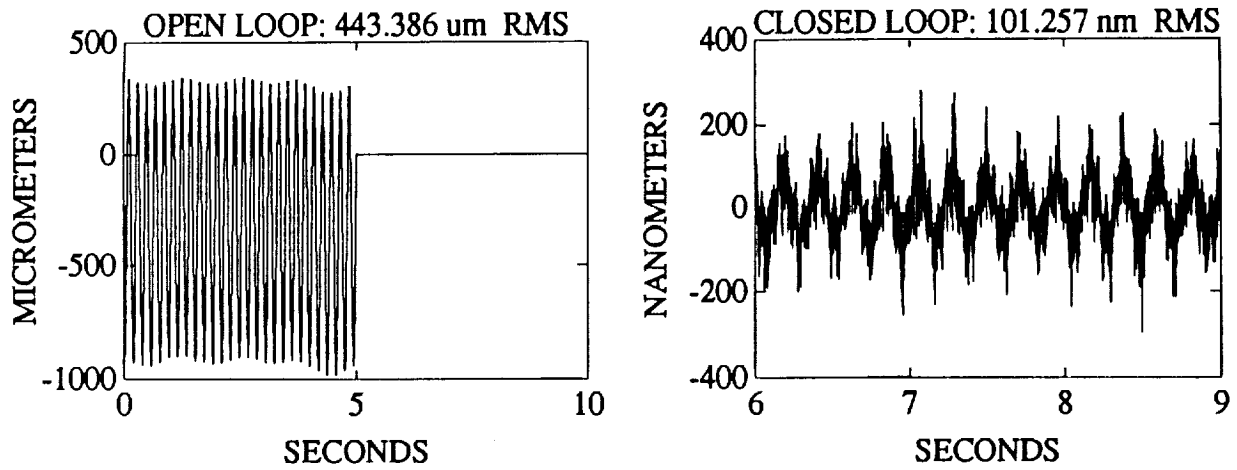# SINUSOID TUNED TO FREQUENCY OF FIRST STRUCTURAL MODE

Figure 10. Closed Loop Optical Performance with Shaker Induced Sinusoidal Disturbance